Proceedings of the 2025 SICE Festival with Annual Conference
September 9-12, 2025, Chiang Mai, Thailand

Self-Localization Using Landmarks in a Small Home Appliance Scrap Yard

Kazuki Oi[1†], Hiroshi Kobayashi[2], Takuya Hashimoto[3], and Ryuzo Hayashi[4]

[1]Graduate School of Engineering, Tokyo University of Science, Japan
(Tel: +81-3-5876-1718; E-mail: kazuki@kobalab.com)
[2]Graduate School of Engineering, Tokyo University of Science, Japan
(Tel: +81-3-5876-1718; E-mail: hiroshi@kobalab.com)
[3]Graduate School of Engineering, Tokyo University of Science, Japan
(Tel: +81-3-5876-1718; E-mail: tak@rs.tus.ac.jp)
[4]Graduate School of Engineering, Tokyo University of Science, Japan
(Tel: +81-3-5876-1718; E-mail: hayashi@rs.tus.ac.jp)

Abstract: As global resource demand and environmental issues escalate, transitioning to a circular economy is essential. This study, part of a NEDO project, develops an autonomous sorting system for electronic waste in home appliance scrap yards. Traditional localization methods like SLAM and GNSS struggle in dynamic environments. To address this, we propose an artificial landmark-based approach. The system uses vertically stacked geometric landmarks, enabling robust detection and self-localization within a 30 m range. Experiments confirm that localization accuracy improves when landmarks are spaced further apart. Future work will focus on reducing detection errors and stabilizing performance in scrap yards. Additionally, we will implement a switching mechanism that uses either camera images alone or a combination of LiDAR and images based on landmark distance.

Keywords: Robotic and Automation Systems, Signal and/or Image Processing, Mechanical Systems Control

1. INTRODUCTION

With the global increase in resource demand and the intensification of environmental issues such as global warming, the transition from a linear economic model to a circular economy has become an urgent matter. In a project commissioned by NEDO [1], we are developing a system that autonomously sorts discarded small home appliances in scrap yards, aiming to effectively utilize the resources contained within these appliances and contribute to the realization of a circular economy.

The system is designed to autonomously navigate, pick up, and sort small appliances, with the goal of being deployable in a variety of existing scrap yards approximately 30 meters square in size. To achieve this, a stable and accurate self-localization capability is essential. However, commonly used SLAM-based localization methods [2] are not suitable for scrap yards due to frequent and unpredictable changes in the surrounding geometry caused by the inflow of discarded appliances. Similarly, localization methods based on GNSS or beacons [3] do not offer sufficient stability and precision for the autonomous sorting system to function reliably.

To address these issues, we propose a self-localization method based on artificial landmarks installed in the environment. We developed a system capable of detecting the positions of these landmarks and estimating the robot's own position accordingly. This paper reports on the design and evaluation of the system, including the proposed landmark structure and its detection mechanism.

† Kazuki Oi is the presenter of this paper.

2. OVERVIEW OF THE SELF-LOCALIZATION SYSTEM

2.1 Landmark Design

In this study, we propose a novel landmark-based approach for self-localization in dynamic environments like home appliance scrap yards. Fig. 1 illustrates the typical layout and the strategic placement of landmarks within such a facility. The scrap yard, approximately 30 meters square in size, requires a minimum of 6 distinct landmark patterns to ensure stable localization and sorting operations. Specifically, this includes at least one landmark on each side of the scrap pile (total 2) and one at each of the three unloading points (total 4), as indicated by landmarks 1-6 in Fig. 1.

Fig. 2 shows the novel landmark design proposed in this study. The landmark consists of vertically stacked three-dimensional shapes: two types of cones (inverted and upright) and a sphere. Due to their rotational symmetry, the shapes appear as triangles and circles in camera images, regardless of viewing angle. Because three distinct shapes are used and stacked vertically, landmark IDs can be assigned using a ternary number system. For example, with two stacked shapes, $3^2 = 9$ unique patterns can be created; with three shapes, $3^3 = 27$ patterns are possible.

Our initial design utilizes two stacked shapes, providing 9 unique patterns. This decision is based on the operational requirements of the target home appliance scrap yard, which sufficiently exceeds the minimum requirement for landmark patterns. For future applications in larger or more complex environments, the system can be readily scaled by increasing the number of

stacked shapes to generate more unique landmark patterns, allowing for a higher density or wider coverage of landmarks as needed.

Regarding the impact of different landmark patterns on recognition and self-localization accuracy, no significant differences in recognition rates or position estimation errors have been confirmed among the various patterns tested so far. However, the possibility that certain patterns may be more prone to misidentification than others, particularly in complex real-world environments, will be investigated in future work using the actual experimental setup. We will also examine whether recognition rates vary significantly within specific distance ranges, as this could impact on the overall localization performance.

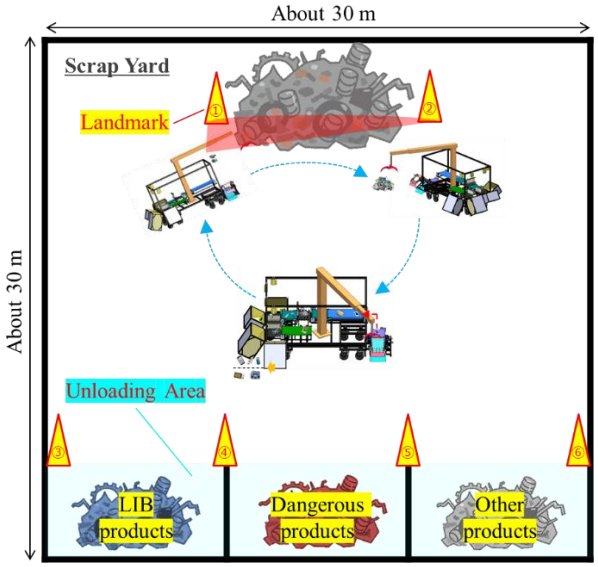

Fig.1 Placement of landmarks

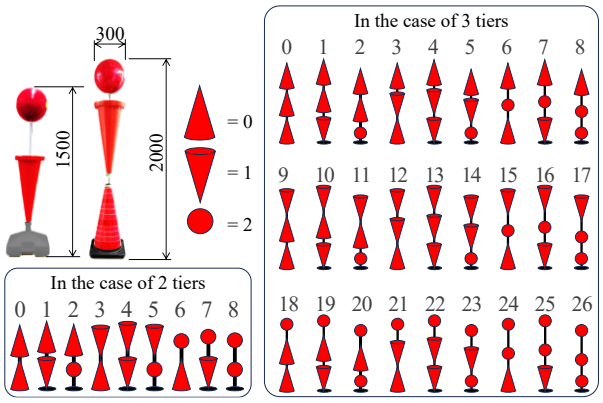

Fig.2 Developed landmark

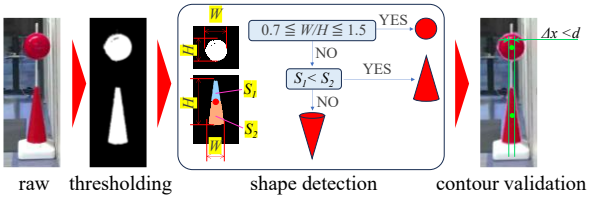

Fig.3 Detection of Landmark

The system then computes the centroid of each extracted shape and checks if the horizontal displacement Δx between centroids is within a predefined threshold d, implying vertical alignment. If this condition is met, the shapes are treated as a landmark. The IDs are assigned by reading the sequence of shapes from top to bottom as digits of a base-3 number, with cone, the inverted cone and sphere, corresponding to values of 0, 1, and 2, respectively.

2.3 Landmark Position Estimation

As illustrated in Fig. 4, landmark positions are estimated by projecting LiDAR point clouds onto the camera image and calculating the average position of points within the red regions detected as landmark components. To reduce false detections and calibration errors, the point cloud is filtered according to three criteria: whether points lie within the colored region, whether the distance corresponds to the expected size based on the red area, and whether the 3D distances between shape centroids match the expected pattern.

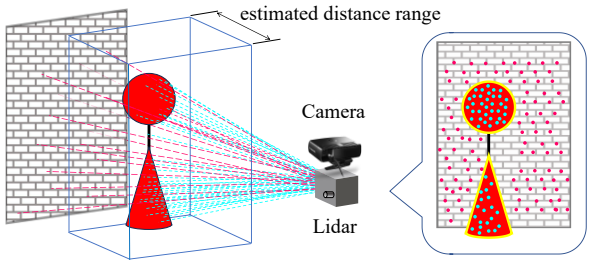

Fig.4 Landmark pose estimation

2.4 System Architecture

Fig 5 shows the overall architecture of the landmark position detection system. This system was implemented using ROS 2, with the use of multiple LiDAR sensors and cameras in mind, and the program was divided into modules. For modules that frequently exchange large amounts of data, such as image processing and Lidar point cloud projection processing, we use container-based process-internal communication. For other communications, we employ asynchronous inter-process communication. To ensure scalability, all data being communicated is stamped with a timestamp, enabling synchronized processing even for data obtained via asynchronous communication based on the time stamp.

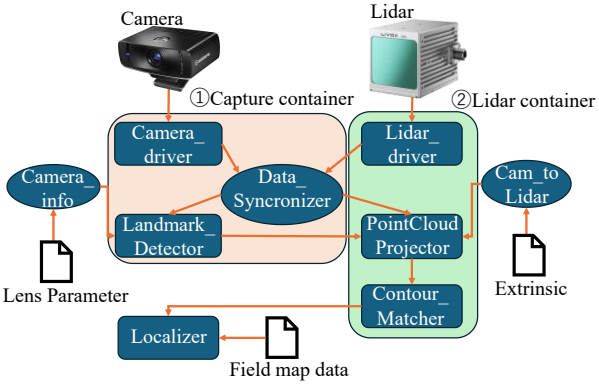

Fig.5 Landmark detection system

2.5 SELF-LOCALIZATION METHOD

The proposed self-localization method utilizes a predefined map that specifies the absolute positions of landmarks in the environment. During operation, the system detects the landmark positions from sensor data and matches them with predefined landmark IDs.

To estimate the robot's pose, we calculate a rigid body transformation that minimizes the error between the detected and predefined landmark positions using singular value decomposition (SVD).

3. DEVELOPMENT OF THE LANDMARK POSITION DETECTION SYSTEM

3.1 Integration of Images and Point Clouds

Accurate localization of the landmarks requires precise integration of image and point cloud data. The camera parameters, including the optical center and focal length, were calibrated using Zhang's chessboard method [4]. The spatial relationship between the camera and LiDAR was estimated using the method proposed by Koide et al. [5], which leverages SuperGlue and Normalized Information Distance (NID).

However, it was found that simply projecting point clouds using camera parameters and sensor positions causes a delay between the image and the point cloud data when the system is operated on actual equipment, resulting in low landmark position detection accuracy during device movement.

To address this, we added timestamps to both the camera and LiDAR data streams. The system incorporates a Data Synchronizer module that ensures synchronization with a maximum allowable time offset of 30 milliseconds between sensors, improving integration accuracy during motion [6].

3.2 Countermeasures Against False Landmark Detection

To ensure robustness in various environments with differing lighting conditions and distances to the landmarks, we redundantly configured thresholds for red color extraction and spatial relationships between shape components. As a result, some non-landmark red objects were occasionally misidentified as landmarks.

These false positives were categorized into two types and comprehensively addressed:

The first case involved instances where the apparent size of a detected object was either too large or too small compared to the actual distance to the landmark. To counter this, we introduced Eq. (1) to estimate the distance D [m] to the landmark based on the red area s [px²] in the image and subsequently used Eq. (2) to identify valid point cloud data, thereby accounting for lighting-induced variations in perceived size. Here, r [m] is the radius of the spheres or cones, f [px] is the focal length in pixels, and Δt [px²] is the error tolerance in area estimation.

The second case addressed situations where the shape of a detected object was inappropriate as a landmark, even if its distance and apparent size were reasonable. Even when size and distance are appropriate, the shape layout might not conform to a valid landmark. In this scenario, we utilized the distances between centroids of the red regions to estimate landmark distance using Eq. (3) and applied thresholding as per Eq. (4) to rigorously reject improper candidates.

Through the implementation of these measures, the phenomenon of false detection points was effectively eliminated.

$$D(s) = r\sqrt{1+\frac{\pi f^2}{s}} \tag{1}$$

$$r\sqrt{1+\frac{\pi f^2}{s+\Delta t/D}} < D < r\sqrt{1+\frac{\pi f^2}{s-\Delta t/D}} \tag{2}$$

$$D(s) = \frac{rf^2}{s} \tag{3}$$

$$\frac{rf^2-\Delta t}{s} < D < \frac{rf^2+\Delta t}{s} \tag{4}$$

As depicted in Fig. 6, non-landmark red areas, which previously caused misidentification, are no longer observed in the detection results after applying these countermeasures. This demonstrates a significant improvement in the reliability of landmark identification.

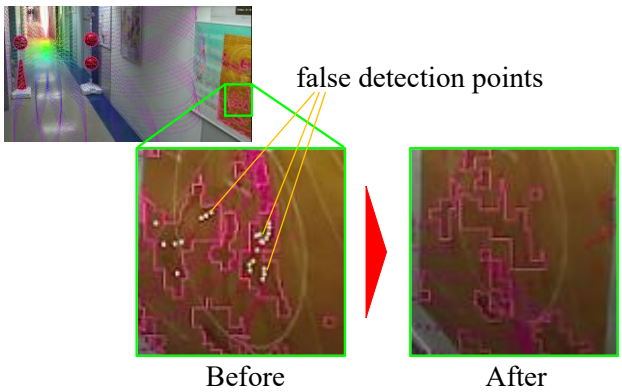

Fig.6 Reduction of false detection points

4. VERIFICATION OF THE SELF-LOCALIZATION SYSTEM

4.1 Experimental Overview

To evaluate whether the developed system could accurately detect landmarks and estimate the robot's self-position in real-world conditions, we conducted verification experiments using actual hardware.

The test platform was the Ranger Mini 3.0 omni-directional mobile robot by AgileX. The vision system comprised an Elgato Facecam Pro camera, while distance measurements were obtained using a Livox Avia LiDAR sensor.

4.2 Experimental Setup

As illustrated in Fig. 7, two landmarks were placed in the field. The robot, equipped with both camera and LiDAR, was moved linearly along the y-axis while

attempting to estimate its position. The robot's x-position was changed from 0 m to 30 m in 5 m increments. The movement range in the y-direction was set to match the distance between the landmarks. The distance between landmarks was set at (a) 1.5 m or (b) 2.5 m.

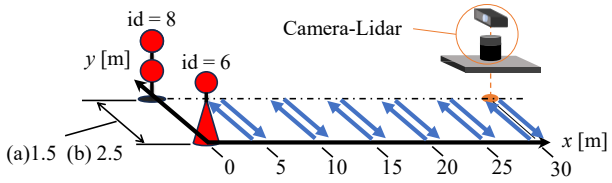

Fig.7 Experimental conditions

4.3 Experimental Results

The self-localization results for the two inter-landmark distances are shown in Fig. 8(a) and (b). For the 1.5 m and 2.5 m cases, the accuracy of the robot's estimated trajectory was compared against the actual path.

4.4 Discussion

From the results in Fig. 8, it can be observed that the estimated trajectory in the 2.5 m landmark distance case more closely matches the actual robot trajectory compared to the 1.5 m case. This improvement in accuracy is attributed to the following factor. Let L[m] be the distance between landmarks and Δx [m] the displacement in the x-direction. The angular error θ [rad] in pose estimation is given by:

$$\varepsilon_\theta = atan(\varepsilon_x / L) \qquad (5)$$

In the case shown in Fig. 8(b), the wider landmark spacing of 2.5 m reduces the impact of error on angular estimation, resulting in improved overall accuracy.

In future work, we will analyze the quantitative relationship between L and Δx and use it to avoid large pose errors in practical applications. Besides increasing landmark spacing, other ways to improve localization accuracy include using angular information extracted from images to refine pose estimates and incorporating robust estimation methods (such as maximum likelihood estimation) to mitigate the influence of outliers or measurement noise. The outdoor results shown in Fig. 9 generally exhibit lower accuracy compared to the indoor experiments. Although the benefit of increased landmark spacing was also observed in the outdoor tests, the estimated trajectory deviated (curved away from the actual path) when the robot was more than 10 m away from both landmarks. Furthermore, in outdoor environments, the system produced fewer localization data points when the distance between two landmarks is greater than 15 m. This suggests that the current system has difficulty detecting landmarks in images in outdoor environments compared to indoor environments, which may lead to a decrease in self-localization accuracy during autonomous driving.

To investigate this issue, the results of red region extraction at each distance in the outdoor experiment are shown on Fig. 10. These results indicate that the system was able to detect the red landmarks even outdoors and that false detections were not significant in this scenario.

Therefore, we propose the following strategy.

At distances between 0–15 m, perform self-localization using both camera images and LiDAR

At distances between 15–30 m, use the camera image to estimate the direction of the landmark and plan navigation toward the approximate target location.

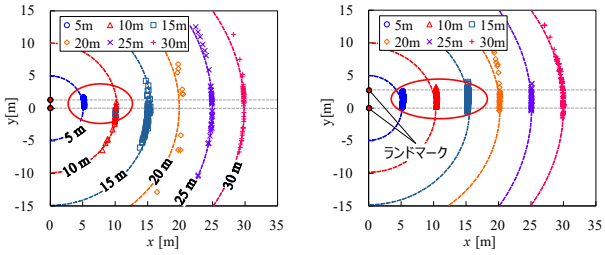

(a) 1.5 m Landmark distance (b) 2.5 m Landmark distance

Fig.8 Result of landmark based localization (indoor)

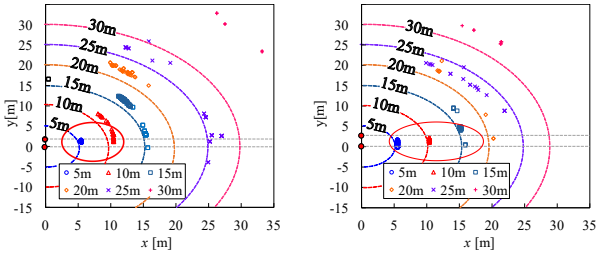

(a) 1.5 m Landmark distance (b) 2.5 m Landmark distance

Fig. 9 Result of Landmark Based Localization (outdoor)

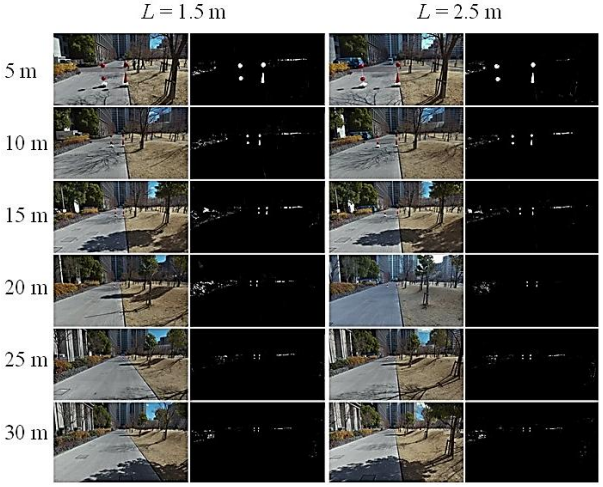

Fig. 10 Result of Thresholding

5. DISCUSSION

In this study, we proposed a novel landmark design and developed a landmark-based self-localization system for an autonomous sorting robot operating in small appliance scrap yards. The system was evaluated through localization experiments conducted within a 30-meter range.

Experimental results demonstrated that the distance between installed landmarks significantly affects localization accuracy, and wider spacing resulted in improved precision. These findings validate the effectiveness of our approach and highlight the importance of spatial configuration in landmark-based

systems.

Future work will focus on reducing errors in landmark position estimation and incorporating techniques that mitigate their influence. Our goal is to achieve a stable and reliable self-localization system that operates effectively even in the variable and cluttered environments of scrap yards. Furthermore, we plan to implement a dynamic switching mechanism that adjusts the self-localization strategy based on the distance to landmarks. At shorter ranges, the system will use both camera images and LiDAR for accurate localization. At longer ranges, it will rely primarily on heading estimation based on landmark centroid position in the camera image to guide navigation.

To address the dynamic nature of scrap yards, where the accumulation of discarded appliances can frequently alter the environment and potentially obscure landmarks, future work will also involve investigating adaptive landmark placement strategies. This includes exploring designs for landmarks that are less prone to being hidden by scrap piles, as well as developing methods for easily re-deploying or adjusting landmark positions as the scrap yard layout changes. Such strategies will contribute to maintaining the continuous visibility and effectiveness of the landmarks in a highly variable setting.

This research was conducted as part of a project commissioned by the New Energy and Industrial Technology Development Organization (NEDO), project number JPNP23002.

REFERENCES

[1] New Energy and Industrial Technology Development Organization (NEDO), “Basic Plan for Development of Core Technologies for Recycling Processes of Waste Electrical and Electronic Equipment toward a Highly Circular System.”

[2] M. Tomono, Y. Hara, “Current Status and Future Prospects of SLAM,” Special Issue on SLAM-based Self-localization Technologies, Vol. 64, No. 2, pp. 45–50, 2020.

[3] S. Tamaki, T. Tanaka, “Consideration of 3D Indoor Location Positioning Technique” Journal of International ICT Application Research Society, Vol. 2, No. 1, pp. 24–30, 2018.

[4] Z. Zhang, “A Flexible New Technique for Camera Calibration,” IEEE Transactions on Pattern Analysis and Machine Intelligence (PAMI), Vol. 22, No. 11, pp. 1330–1334, 2000.

[5] K. Koide, “General, Single-shot, Target-less, and Automatic LiDAR-Camera Extrinsic Calibration Toolbox,” Proceedings of the IEEE International Conference on Robotics and Automation (ICRA), 2023.

[6] Reita Yamagishi et al., “Detection of Landmark Positions in a 30m-Class Small Home Appliance Scrap Yard,” 67th Joint Automatic Control Conference, 2024.